Pan-cancer analysis of *DEPDC1* as a candidate prognostic biomarker and associated with immune infiltration

Boquan Jia[1#], Jun Liu[2#], Xin Hu[3,4,5], Lu Xia[1], Ying Han[1,3]

[1]Center for Medical Genetics & Hunan Key Laboratory of Medical Genetics, School of Life Sciences, Central South University, Changsha, China; [2]Department of Clinical Laboratory, Affiliated Xiaoshan Hospital, Hangzhou Normal University, Hangzhou, China; [3]Department of Oral and Maxillofacial Surgery, Center of Stomatology, Xiangya Hospital of Central South University, Changsha, China; [4]Research Center of Oral and Maxillofacial Tumor, Xiangya Hospital of Central South University, Changsha, China; [5]Institute of Oral Cancer and Precancerous Lesions, Central South University, Changsha, China

Contributions: (I) Conception and design: Y Han; (II) Administrative support: None; (III) Provision of study materials or patients: None; (IV) Collection and assembly of data: B Jia, J Liu; (V) Data analysis and interpretation: B Jia, J Liu; (VI) Manuscript writing: All authors; (VII) Final approval of manuscript: All authors.

[#]These authors contributed equally to this work and should be considered as co-first authors.

Correspondence to: Ying Han. Center for Medical Genetics & Hunan Key Laboratory of Medical Genetics, School of Life Sciences, Central South University, Changsha 410008, China. Email: hanying@sklmg.edu.cn.

Background: DEP domain containing 1 (DEPDC1) gene is upregulated in several malignancies and contributes to tumorigenesis. Although the role of DEPDC1 in tumor is becoming increasingly popular, the function of DEPDC1 in pan-cancer still needs to be systematically elucidated.

Methods: Data were downloaded from Genotype-Tissue Expression Data (GTEx), The Cancer Genome Atlas (TCGA) TIMER2.0, TISIDB, STRING, and CancerSEA databases and analyzed to determine the functionality of the *DEPDC1*. The results were visualized using tools provided by the databases and the R language.

Results: The results showed that *DEPDC1* was significantly upregulated in 29 of the 33 human cancers analyzed. In addition, there were significant differences in *DEPDC1* expression among cancer immune and molecular subtypes. Gene Ontology (GO) and Kyoto Encyclopedia of Genes and Genomes (KEGG) analysis showed that *DEPDC1* was mainly involved in the cell cycle, and CancerSEA analysis showed that *DEPDC1* promoted cell cycle, DNA repair, DNA damage, and proliferation in pan-cancer. Receiver operating characteristic (ROC) curve analysis showed high predictive accuracy for pan-cancer. *DEPDC1* expression was positively correlated with activated CD4^{+} T helper 2 cells and common lymphoid progenitor cells, and negatively correlated with natural killer (NK) T cells, CD4^{+} central memory T cells, and CD4^{+} effector memory T cells. Furthermore, *DEPDC1* was significantly positively correlated with T cell exhaustion marker genes, such as *CD274*, transforming growth factor beta receptor 1 (TGFBR1), kinase insert domain receptor (KDR), programmed cell death 1 ligand 2 (PDCD1LG2), granzyme B (*GZMB*), and granulysin (*LAG2*). Additionally, *DEPDC1* was associated with overall survival (OS), disease-specific survival (DSS), and progress-free interval (PFI) prognosis in multiple tumor types. The ROC analysis showed high predictive accuracy for pan-cancer.

Conclusions: Collectively, *DEPDC1* is aberrantly expressed and plays an immune-oncogenic role in pan-cancer, and *DEPDC1* may serve as a biomarker for cancer diagnosis and therapy.

Keywords: *DEPDC1*; prognostic; pan-cancer; immune infiltration; immune checkpoints

Introduction

Cancer is the second leading cause of death globally after ischemic heart disease, but is predicted to become the leading cause of death in 2060 (1). In 2021, there were 1,898,160 new cases of cancer and approximately 610,000 deaths in the United States (2). Despite decades of tremendous progress in multiple oncological treatment strategies (3), the efficacy of currently available therapies remains poor. The past decade has witnessed dramatic advances in cancer treatment through immunotherapy (4). The human immune system is an important barrier for preventing the occurrence and development of tumors. Unfortunately, cancer cells have evolved multiple strategies to evade the immune system, which has slowed the development of cancer immunotherapy strategies (5-7). Identifying biomarkers with the potential to respond to immunotherapy and understanding the roles of these markers may guide the clinical development of immunotherapy strategies for patients with cancer (8).

DEPDC1 is encoded by DEP domain containing 1, which is located in the 1p31.3 region of human chromosome 1. *DEPDC1* is a newly reported novel tumor-related gene that is upregulated in several malignancies and has been shown to contribute to the tumorigenesis of various tumors, such as lung (9-11), gastric (12), hepatocellular (13-15), bladder (16,17), breast (18), prostate (19) and colorectal cancer (CRC) (20). Interestingly, *DEPDC1* has almost undetectable expression in the other normal human tissues, with the exception of the testes (17,21). Harada *et al.* demonstrated that *DEPDC1* can directly interact with zinc finger

protein *ZNF224* to form a complex, thereby inhibiting the transcription of A20, resulting in the activation of anti-apoptotic pathways after nuclear factor kappa B *(NFkB)* translocation to the nucleus (16). Feng *et al.* showed that *DEPDC1* is essential for acceleration of nasopharyngeal carcinoma cell motility and cycle progression (22). In addition, *DEPDC1* promoted CRC proliferation, migration, and invasion through the regulation of SUZ12-mediated H3K27Me3 (20). However, the precise role of *DEPDC1* in pan-cancer has not been reported, and the role of *DEPDC1* in immune infiltration remains to be fully elucidated.

This current study investigated the expression of *DEPDC1* in patients with pan-cancer and examined its association with patient prognosis. We further analyzed the association between *DEPDC1* and the immune cell infiltration and immune inhibitor genes. The results herein provide novel insights into the functional role of *DEPDC1* in pan-cancer, highlighting a potential mechanism whereby *DEPDC1* influences the tumor microenvironment, as well as cancer immunotherapy. This project systematically studies the expression, mutation, prognosis, and function of DEPEC1 in human pan-cancers, providing a broad-spectrum biomarker for cancer diagnosis and treatment. We present the following article in accordance with the REMARK reporting checklist (available at https://atm.amegroups.com/article/view/10.21037/atm-22-5598/rc).

Methods

Mutation profiles

The cBioPortal for cancer genomics (http://www.cbioportal.org) is an open-access repository of cancer genomics datasets (23,24). The cBioPortal database was used to analyze DEPDC1 genomic changes in order to analyze DEPDC1 mutations in pan-carcinoma.

Data collection

The RNA expression profiles and clinical data of 33 tumor types and 15,776 normal tissues samples were download from The Cancer Genome Atlas (TCGA) database and the Genotype-Tissue Expression (GTEx) database from the UCSC Xena database (http://xena.ucsc.edu/). To comprehensively investigated differential expression levels of *DEPDC1* between tumor and adjacent normal tissues across TCGA cancer types, the Wilcoxon rank-sum test

---

Highlight box

Key findings
- DEPDC1 is abnormally upregulated in pan-carcinoma tissues, and its expression is significantly different in immune subtypes and molecular subtypes of various tumors, which also has excellent diagnostic and prognostic value. Its main functions are to regulate cell cycle, proliferation, DNA damage and repair, and also to inhibit immune infiltration.

What is known and what is new?
- DEPDC1 is a newly reported tumor-associated gene.
- DEPDC1 is overactivated and expressed in pan-cancer and is also significantly positively correlated with many immune checkpoints.

What is the implication, and what should change now?
- DEPDC1 can be used as a broad-spectrum biomarker for the diagnosis and therapeutic of pan-cancer.

---

was performed, and P<0.05 was considered statistically significant (ns, P≥0.05; *P<0.05; **P<0.01; ***P<0.001) (25).

Protein-protein interaction networks

The STRING (https://string-preview.org/) database was used to analyze the protein interaction network of *DEPDC1* and to obtain interacting genes and proteins.

Kyoto Encyclopedia of Genes and Genomes enrichment analysis and Gene Ontology

The Kyoto Encyclopedia of Genes and Genomes (KEGG) enrichment analyses and Gene Ontology (GO) was conducted for 50 *DEPDC1*-binding proteins using the ggplot2 package for visualization and the cluster Profiler package for statistical analysis.

Immune cell infiltration

TIMER is a comprehensive resource for systematical analysis of immune infiltrates across diverse cancer types (26,27). TIMER 2.0 (http://timer.cistrome.org/) was used to analyze the correlation of *DEPDC1* expression levels with the infiltration levels of 34 immune cell types associated with pan-cancer in the XCELL webtool (28). A P value <0.05 was considered statistically significant.

Analysis of the immune and molecular subtypes associated with DEPDC1 in pan-cancer

The TISIDB database, an integrated repository portal for tumor-immune system interactions (29) (http://cis.hku.hk/TISIDB/index.php), was used to explore the correlations between *DEPDC1* expression and immune subtypes or molecular subtypes in pan-cancer. A P value <0.05 was considered statistically significant.

Analysis of the prognostic and diagnostic value of DEPDC1

Univariate Cox regression analyses of *DEPDC1* and clinical characteristics were conducted to assess its prognostic value in the overall survival (OS), disease specific survival (DSS), and progress-free interval (PFI) of pan-cancer patients. The receiver operating characteristic (ROC) curve was used to assess the diagnostic value of *DEPDC1* in pan-cancer.

Single-cell analysis

CancerSEA is the first dedicated database aimed at comprehensively decoding the functional status of cancer cells at a single-cell resolution. CancerSEA (30) (http://biocc.hrbmu.edu.cn/CancerSEA/home.jsp) was used to explore *DEPDC1* family-expressed functions.

Oral squamous cell carcinoma samples and immunohistochemical staining of DEPDC1

From 2018 to 2019, a total of 57 oral squamous cell carcinoma (OSCC) samples and 12 normal healthy oral tissue samples were collected at Xiangya Hospital (the affiliated hospital of Central South University) in Changsha, Hunan. The inclusion and exclusion criteria of the OSCC patients and the construction of tissue microarray have been detailed in our previous study (31). Immunohistochemistry (IHC) was performed, as previously described (31), to evaluate the expression level of the *DEPDC1* protein, using an anti-*DEPDC1* antibody (Abcam, ab197246, 1:300). Negative controls, positive controls, and phosphate buffered saline (PBS) blank controls were used to determine the efficacy of the IHC staining. The study was conducted in accordance with the Declaration of Helsinki (as revised in 2013). The study was approved by the Ethics Committee of School of Life Sciences, Central South University (No. 2022-1-44) and informed consent was taken from all the patients.

Statistical analyses

The R (v.3.6.3) software was used for data visualization. GraphPad 8.0 was used for statistical analysis of the data. The Wilcoxon rank-sum test or Student's t-test was performed for comparisons between groups. Correlation analysis was conducted using Pearson or Spearman's test as appropriate. Survival analysis was performed using univariate Cox regression, with P<0.05 being considered statistically significant.

Results

Analysis of DEPDC1 expression in pan-cancer

An unpaired analysis of *DEPDC1* expression in pan-cancer revealed a significant upregulation of *DEPDC1* in numerous cancers, including adrenocortical carcinoma (ACC), bladder urothelial carcinoma (BLCA), breast invasive carcinoma

(BRCA), cervical squamous cell carcinoma and endocervical adenocarcinoma (CESC), cholangiocarcinoma (CHOL), colon adenocarcinoma (COAD), lymphoid neoplasm diffuse large B-cell lymphoma (DLBC), esophageal carcinoma (ESCA), glioblastoma multiforme (GBM), head and neck squamous cell carcinoma (HNSC), kidney chromophobe (KICH), kidney renal clear cell carcinoma (KIRC), kidney renal papillary cell carcinoma (KIRP), brain lower grade glioma (LGG), liver hepatocellular carcinoma (LIHC), lung adenocarcinoma (LUAD), lung squamous cell carcinoma (LUSC), ovarian serous cystadenocarcinoma (OV), pancreatic adenocarcinoma (PAAD), pheochromocytoma and paraganglioma (PCPG), prostate adenocarcinoma (PRAD), rectum adenocarcinoma (READ), sarcoma (SARC), skin sutaneous melanoma (SKCM), stomach adenocarcinoma (STAD), thyroid carcinoma (THCA), thymoma (THYM), yterine corpus endometrial carcinoma (UCEC), and uterine carcinosarcoma (UCS). In contrast, *DEPDC1* was significantly downregulated in acute myeloid leukemia (LAML) and testicular germ cell tumors (TGCT) (*Figure 1A*). A paired analysis of *DEPDC1* expression in pan-cancer showed that DEPDC1 was significantly upregulated in BLCA, BRCA, CHOL, COAD, ESCA, HNSC, KICH, KIRC, KIRP, LIHC, LUAD, LUSC, STAD, and UCSC, but did not change in PAAD, PRAD, READ, and THCA (*Figure 1B*). In addition, *DEPDC1* expression was highest in TCGA tumor tissues in ESCA, CESC, and SARC (*Figure 1C*). However, the expression of *DEPDC1* was at a lower level in all other normal tissues, except in the normal tissues of LAML and TGCT (*Figure 1D*).

Correlations between DEPDC1 and immune subtypes of pan-cancer

Differentiating immune subtypes of tumors is of great clinical value for precision medicine of tumors (32). To determine the correlation of *DEPDC1* gene expression with immune subtypes in pan-cancer, we explored the differential *DEPDC1* expression in pan-cancer immune subtypes, namely, C1: wound healing; C2: interferon gamma (*IFN-g*) dominant; C3: inflammatory; C4: lymphocyte depleted; C5: immunologically quiet; and C6: tumor growth factor beta (*TGF-b*) dominant, from the TISIDB database. The outcomes of immune subtypes showed that *DEPDC1* was lowest in C3 subtypes of BLCA (*Figure 2A*), BRCA (*Figure 2B*), COAD (*Figure 2C*), ESCA (*Figure 2D*), LIHC (*Figure 2E*), LUAD (*Figure 2F*), LUSC (*Figure 2G*), MESO (*Figure 2H*), OV (*Figure 2I*), PAAD (*Figure 2J*), PRAD

(*Figure 2K*), READ (*Figure 2L*), SARC (*Figure 2M*), SKCM (*Figure 2N*), STAD (*Figure 2O*), TGCT (*Figure 2P*), THCA (*Figure 2Q*), and UCEC (*Figure 2R*). In addition, the expression of DEPDC1 was the lowest in the C5 immune subtypes of tumors including ACC (*Figure 2S*), GBM (*Figure 2T*), KIRC (*Figure 2U*), KIRP (*Figure 2V*), and LGG (*Figure 2W*).

Correlations between DEPDC1 and molecular subtypes of pan-cancer

Meanwhile, significant differences exist in the expression of *DEPDC1* in different molecular subtypes. The results indicated that the expression of *DEPDC1* in C2c-CpG island methylator phenotype (CIMP) is highest in KIRP relative to other molecular subtypes (*Figure 3A*). In BRCA, *DEPDC1* was highest expressed in the molecular subtype of basal (*Figure 3B*). In COAD, *DEPDC1* was highest expressed in the molecular subtype of Hypermutated- single nucleotide variants (HM-SNV) (*Figure 3C*). In LUSC, *DEPDC1* was highest expressed in the molecular subtype of primitive (*Figure 3D*). In UCEC, *DEPDC1* was highest expressed in the molecular subtype of copy number high (CN_HIGH) (*Figure 3E*). In LIHC, *DEPDC1* was highest expressed in the molecular subtype of iCluster.2 (*Figure 3F*). In READ, *DEPDC1* was highest expressed in the molecular subtype of Hypermutated (HM)-indel (*Figure 3G*). In STAD, *DEPDC1* was highest expressed in the molecular subtype of HM-indel (*Figure 3H*). In ACC, *DEPDC1* was highest expressed in the molecular subtype of CIMP-high (*Figure 3I*). In OV, *DEPDC1* was highest expressed in the molecular subtype of immunoreactive (*Figure 3J*). In PRAD, *DEPDC1* was highest expressed in the molecular subtype of 6-FOXA1 (*Figure 3K*). In PCPG, *DEPDC1* was highest expressed in the molecular subtype of Wnt-altered (*Figure 3L*). In LGG, *DEPDC1* was highest expressed in the molecular subtype of G-CIMP-low (*Figure 3M*).

The landscape of DEPDC1 mutation profile in different tissues

The cBioPortal was used to examine the mutation frequency of *DEPDC1* in the TCGA pan-cancer atlas (10,967 samples in 32 studies). Endometrial carcinoma was found to have the highest mutation level with the *DEPDC1* alteration frequency exceeding 7% (*Figure 4A*). In addition, the frequency and pattern of genetic alterations in numerous genes was similar to that of DEPDC1 genetic alterations
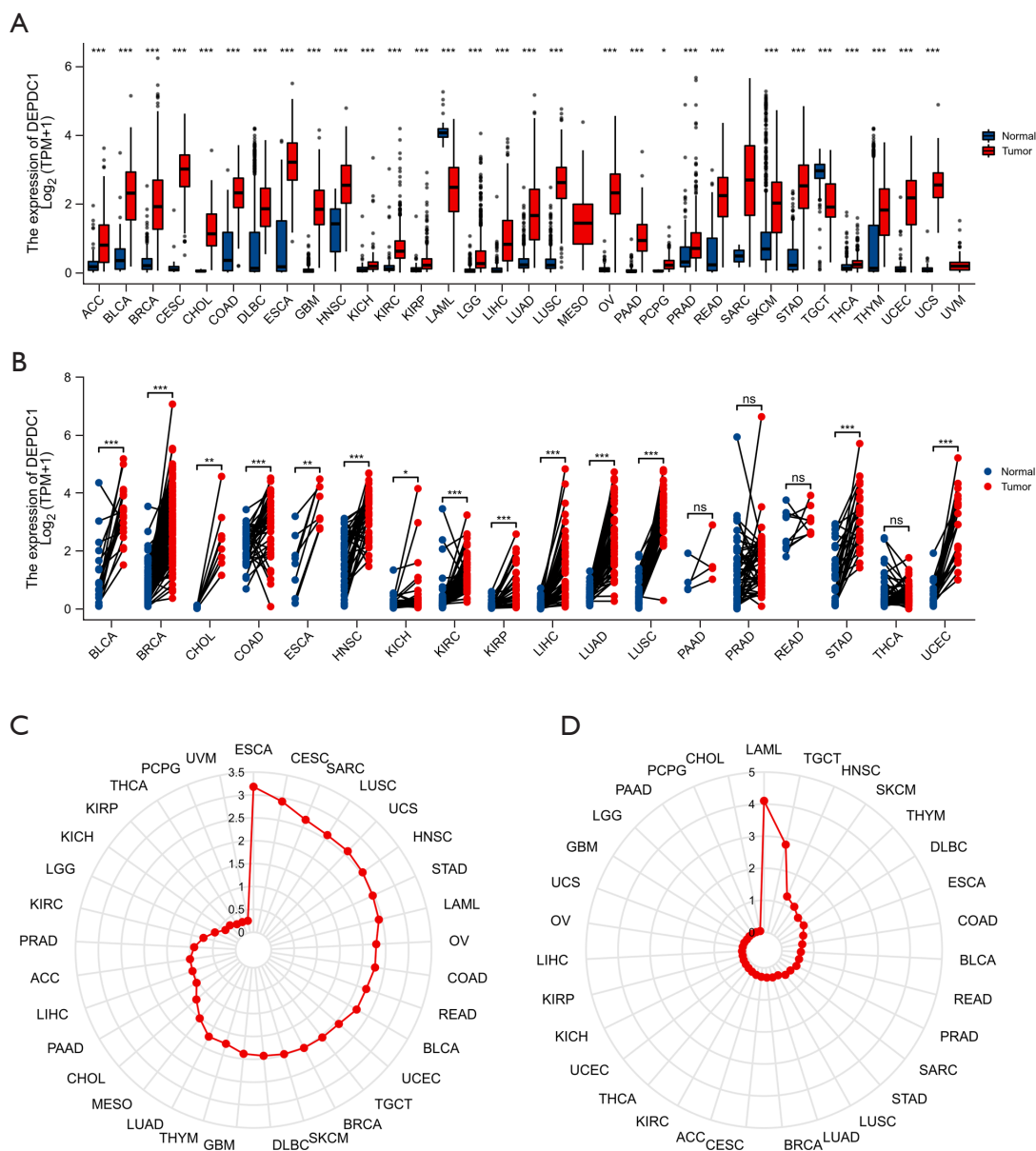
Figure 1 The expression of *DEPDC1* in pan-cancer. (A) Pan-cancer expression of *DEPDC1* between tumor tissues from TCGA database and normal tissues from TCGA and GTEx database. (B) Pan-cancer expression of *DEPDC1* between tumor tissues from TCGA database and adjacent normal tissues. (C) *DEPDC1* expression in tumor tissues from TCGA database. (D) *DEPDC1* expression in normal tissues from TCGA and GTEx database. *P<0.05; **P<0.01; ***P<0.001; ns, not significant. TCGA, The Cancer Genome Atlas; GTEx, Genotype-Tissue Expression.

(*Figure 4B,4C*), including titin (*TTN*), leucine rich repeat containing 7 (*LRRC7*), tumor protein p53 (*TP53*), CUB and Sushi multiple domains 2 (*CSMD*), mucin 16, cell surface associated (*MUC16*), spectrin repeat containing nuclear envelope protein 1 (*SYNE1*), cache domain containing 1

(*CACHD1*), dedicator of cytokinesis 7 (*DOCK7*), DnaJ heat shock protein family (Hsp40) member C6 (*DNAJC6*), and LDL receptor related protein 1B (*LRP1B*). However, *DEPDC1* genetic alterations in the study cohort were not associated with prognostic outcomes (*Figure 4D*).
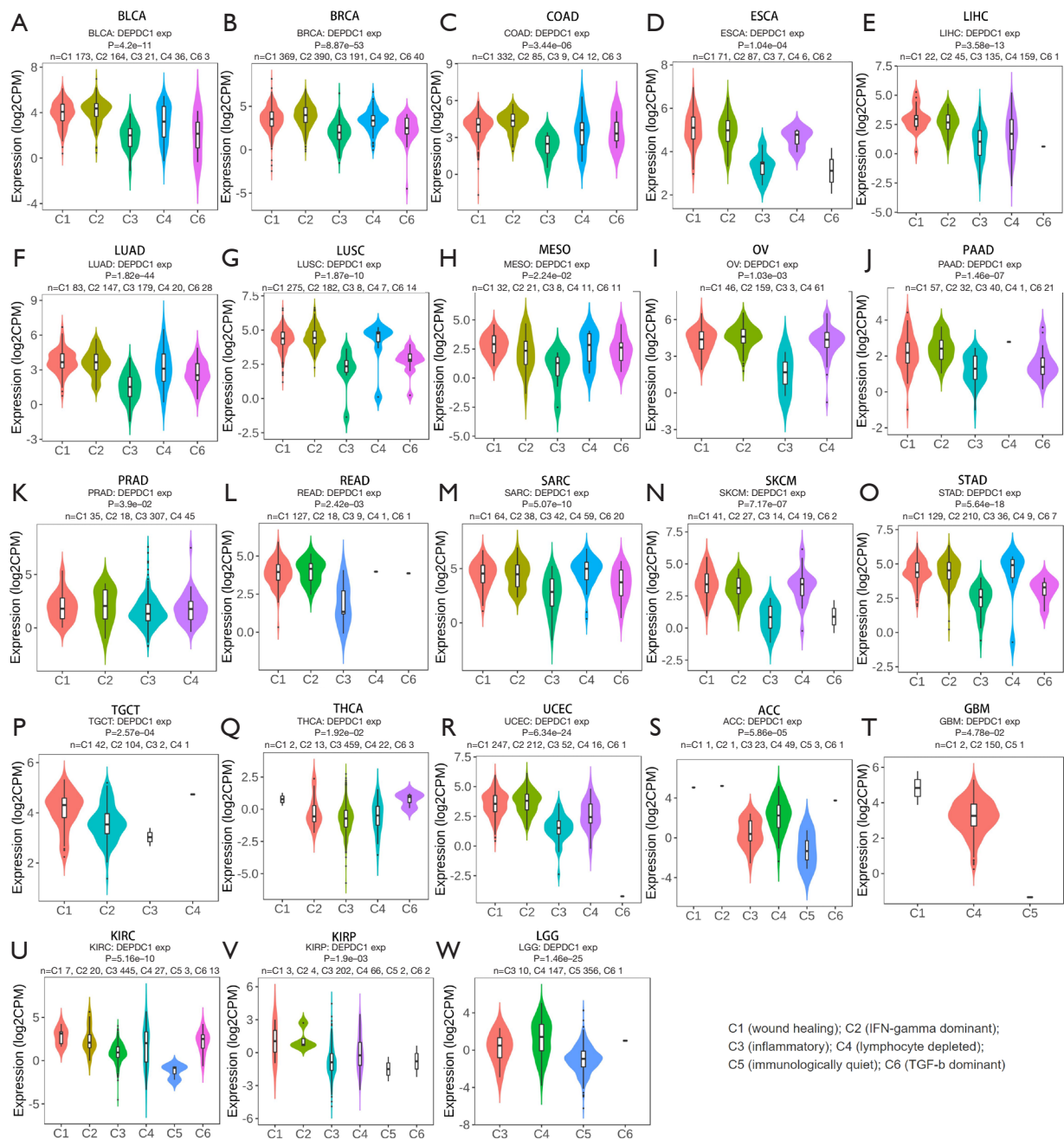
Figure 2 The differential *DEPDC1* expression in pan-cancer immune subtypes. (A) BLCA; (B) BRCA; (C) COAD; (D) ESCA; (E) LIHC; (F) LUAD; (G) LUSC; (H) MESO; (I) OV; (J) PAAD; (K) PRAD; (L) READ; (M) SARC; (N) SKCM; (O) STAD; (P) TGCT; (Q) THCA; (R) UCEC; (S) ACC; (T) GBM; (U) KIRC; (V) KIRP; (W) LGG. BLCA, bladder urothelial carcinoma; BRCA, breast invasive carcinoma; COAD, colon adenocarcinoma; ESCA, esophageal carcinoma; LIHC, liver hepatocellular carcinoma; LUAD, lung adenocarcinoma; LUSC, lung squamous cell carcinoma; MESO, mesothelioma ovarian; OV, ovarian serous cystadenocarcinoma; PAAD, pancreatic adenocarcinoma; PRAD, prostate adenocarcinoma; READ, rectum adenocarcinoma; SARC, sarcoma; SKCM, skin cutaneous melanoma; STAD, stomach adenocarcinoma; TGCT, testicular germ cell tumors; THCA, thyroid carcinoma; UCEC, uterine corpus endometrial carcinoma; ACC, adrenocortical carcinoma; GBM, glioblastoma multiforme; KIRC, kidney renal clear cell carcinoma; KIRP, kidney renal papillary cell carcinoma; LGG, brain lower grade glioma; CPM, counts per million.
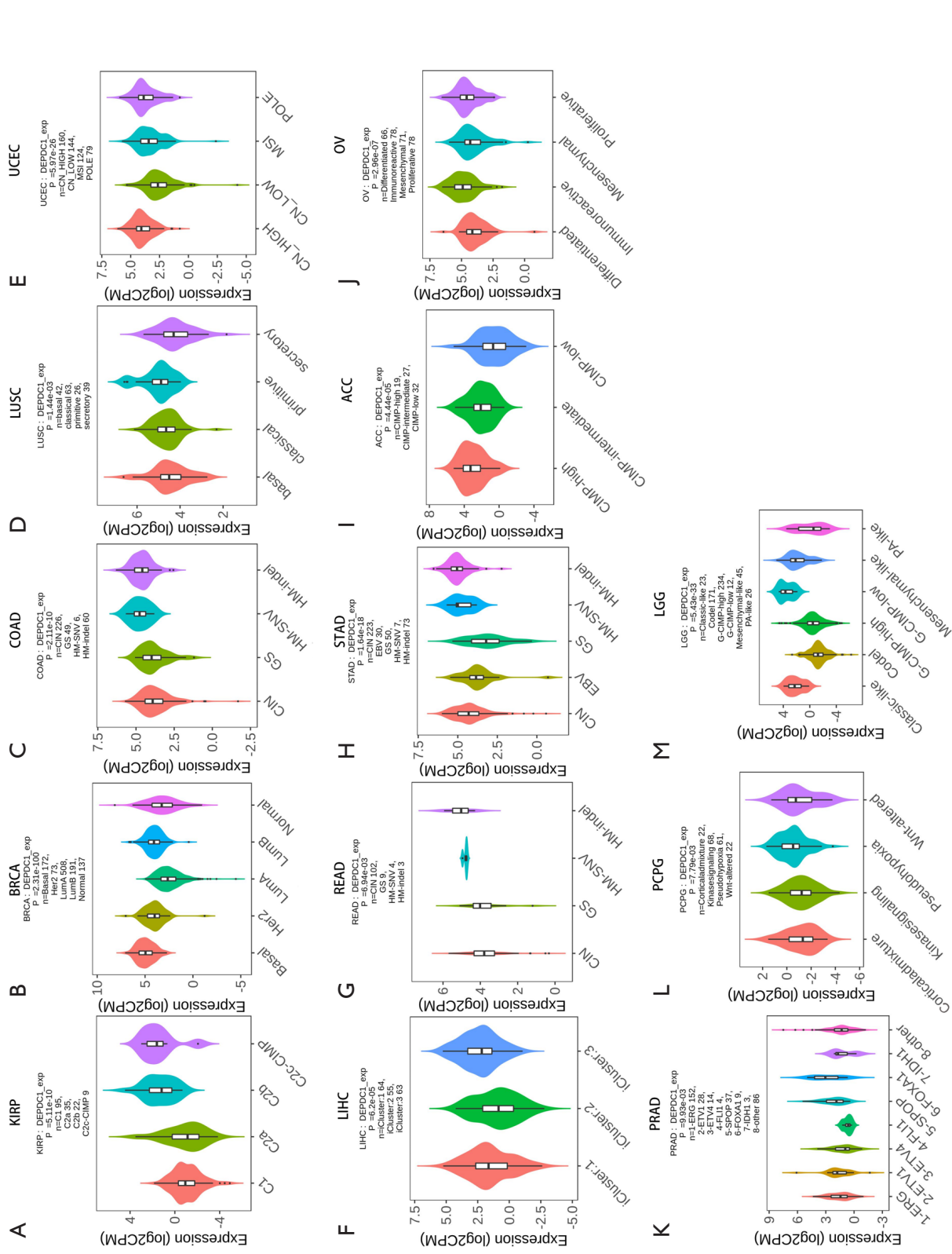
Figure 3 The differential *DEPDC1* expression in pan-cancer molecular subtypes. (A) KIRP; (B) BRCA; (C) COAD; (D) LUSC; (E) UCEC; (F) LIHC; (G) READ; (H) STAD; (I) ACC; (J) OV; (K) PRAD; (L) PCPG; (M) LGG. KIRP, kidney renal papillary cell carcinoma; BRCA, breast invasive carcinoma; COAD, colon adenocarcinoma; LUSC, lung squamous cell carcinoma; UCEC, uterine corpus endometrial carcinoma; LIHC, liver hepatocellular carcinoma; READ, rectum adenocarcinoma; STAD, stomach adenocarcinoma; ACC, adrenocortical carcinoma; OV, ovarian serous cystadenocarcinoma; PRAD, prostate adenocarcinoma; PCPG, Pheochromocytoma and Paraganglioma; LGG, brain lower grade glioma; CPM, counts per million.
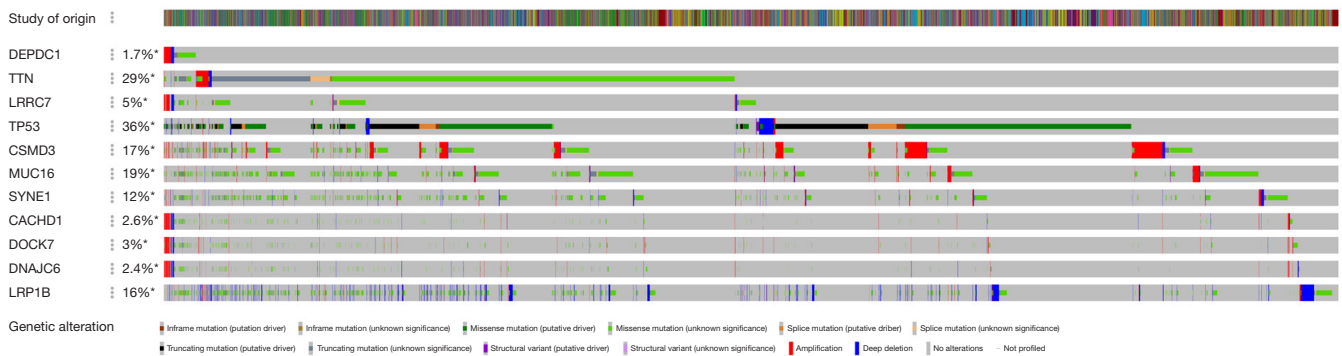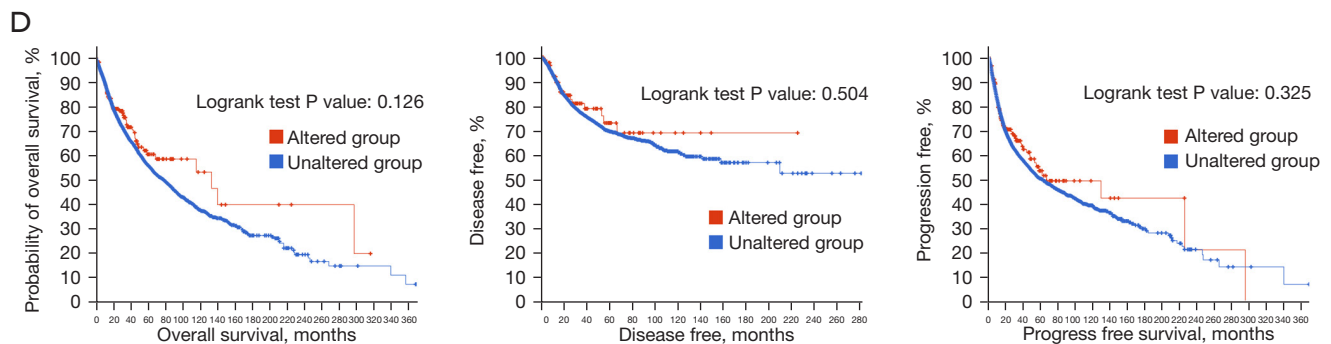
A
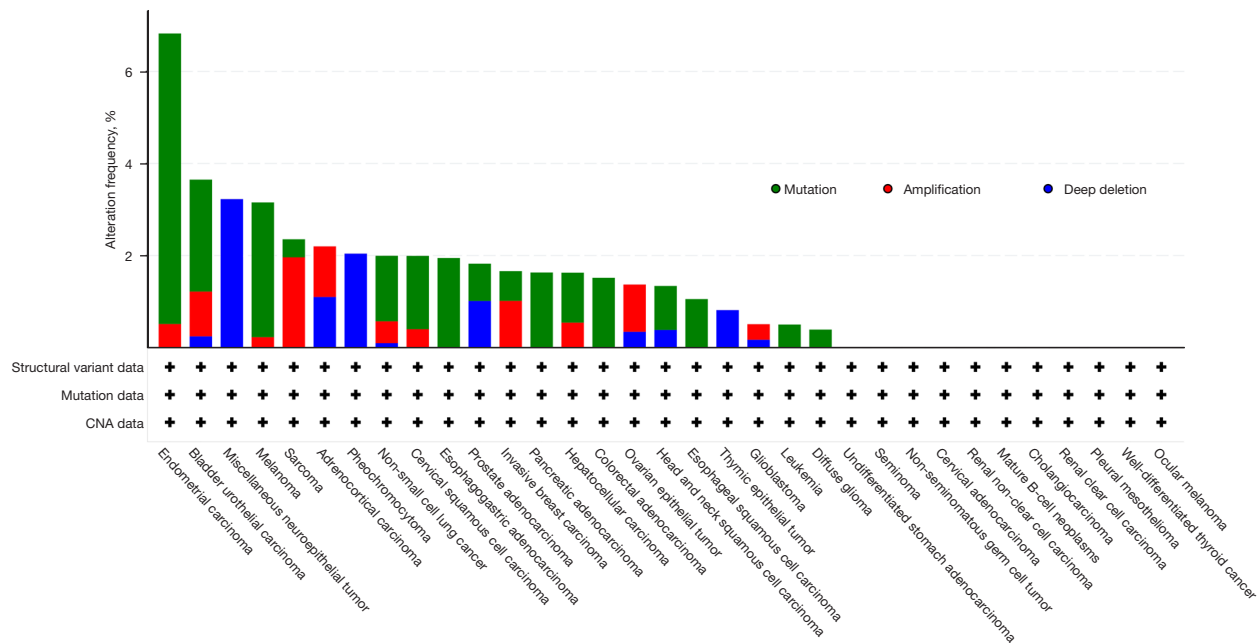
B
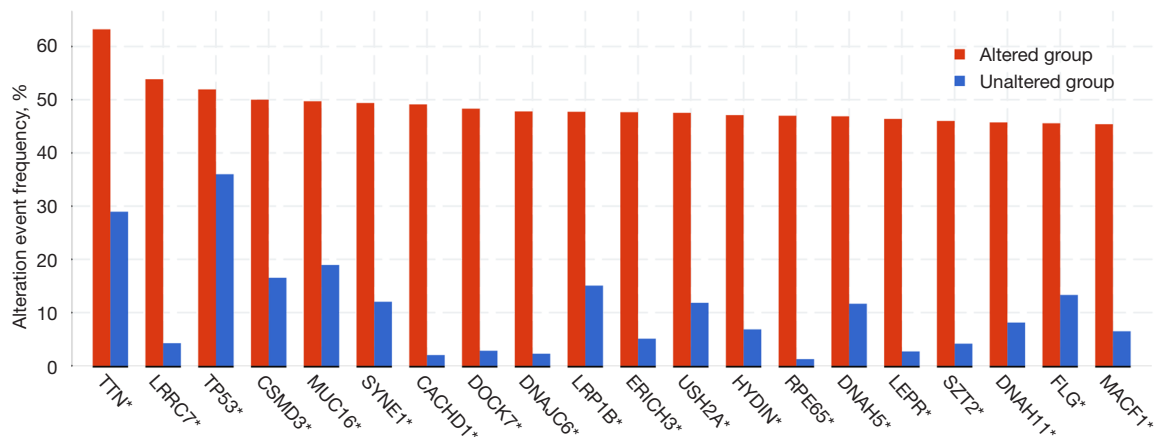
C

Figure 4 Genetic alterations of *DEPDC1*. (A) Co-occurrence of genetic mutations in tumors with *DEPDC1* alterations. (B,C) The association between *DEPDC1* alterations in TCGA pan-cancer atlas studies. * represents a duplicate allele. (D) Kaplan-Meier curves of differences in overall survival, disease-free, and progression-free survival between TCGA pan-cancer atlas studies with altered *DEPDC1* and those without altered *DEPDC1*. TCGA, The Cancer Genome Atlas; CNA, copy number aberration.

Diagnostic value of DEPDC1 in pan-cancer

A ROC analysis of *DEPDC1* in pan-cancer was performed to assess its diagnostic value. The results revealed that *DEPDC1* has diagnostic value in pan-cancer (*Figure 5*), with area under the curve (AUC values) as follows: ACC, AUC =0.811; BLCA, AUC =0.910; BRCA, AUC =0.969; CESC, AUC =0.993; CHOL, AUC =1.000; COAD, AUC =0.951; DLBC, AUC =0.773; ESCA, AUC =0.963; GBM, AUC =0.999; HNSC, AUC =0.891; KICH, AUC =0.717; KIRC, AUC =0.909; KIRP, AUC =0.767; LAML, AUC =0.964; LGG, AUC =0.893; LIHC, AUC =0.928; LUAD AUC =0.946; LUSC, AUC =0.992; OV, AUC =0.997; PAAD, AUC =0.981; PRAD, AUC =0.707; READ, AUC =0.943; SKCM, AUC =0.767; STAD, AUC =0.965; TGCT, AUC =0.832; THCA, AUC =0.690; THYM, AUC =0.754; UCEC, AUC =0.983; and UCS, AUC =1.000. Among them, the prediction accuracy of *DEPDC1* for CESC, CHOL, LUSC, OV, and UCS was greater than 0.99.

Analysis of the prognostic value of DEPDC1 in pan-cancer

To investigate whether *DEPDC1* has potential prognostic value, univariate Cox regression was used to explore the relationship between *DEPDC1* expression and prognosis in multiple tumor types. High *DEPDC1* expression was associated with poor OS in patients with [hazard ratio (HR) =8.22; 95% confidence interval (CI): 2.09–21.87, P<0.001], KIRC (HR =1.52; 95% CI: 1.12–2.07, P=0.007), KIRP (HR= 2.23; 95% CI: 1.20–3.19, P=0.011), LGG (HR =2.1; 95% CI: 2.08–3.61, P<0.001), LIHC (HR =1.82; 95% CI: 1.28–2.58, P=0.001), LUAD (HR =1.5; 95% CI: 1.12–2.00,

P=0.006), MESO (HR =2.97; 95% CI: 2.27–6.63, P<0.001), PAAD (HR =1.88; 95% CI: 1.22–2.86, P=0.002), and UCEC (HR =1.51; 95% CI: 1.00–2.28, P=0.039). Higher *DEPDC1* expression was associated with good OS in cases of COAD [HR =0.57 (0.28–0.85), P=0.005], READ (HR =0.21; 95% CI: 0.08–0.56, P=0.002), and THYM (HR =0.08; 95% CI: 0.01–0.65, P=0.018) (*Figure 6A*). In addition, DSS analysis showed that high *DEPDC1* expression was a marker for poor outcome for patients with ACC (HR= 7.92; 95% CI: 2.95–21.26, P<0.001), KIRC (HR =2.06; 95% CI: 1.38–3.07, P<0.001), KIRP (HR= 9.08; 95% CI: 2.74–30.07, P<0.001), LGG (HR =3.19; 95% CI: 2.10–4.84, P<0.001), LIHC (HR =2.33; 95% CI: 1.47–3.70, P=0.001), LUAD (HR =1.55; 95% CI: 1.07–2.24, P=0.019), MESO (HR =4.57; 95% CI: 2.38–8.77, P<0.001), PAAD (HR =1.9; 95% CI: 1.18–3.06), P=0.008), UCEC (HR =2.16; 95% CI: 1.28–3.65, P=0.004), and UVM (HR =2.64; 95% CI: 1.02–6.82, P=0.045). Higher *DEPDC1* expression was associated with good OS in cases of COAD (HR =0.5; 95% CI: 0.30–0.84, P=0.009) and READ (HR =0.22; 95% CI: 0.06–0.79, P=0.02) (*Figure 6B*). Furthermore, PFI analysis showed that high *DEPDC1* expression was a marker for poor outcome for patients with ACC (HR= 3.91; 95% CI: 1.99–7.67, P<0.001), BLCA; CI (HR =1.35; 95% CI: 1.00–1.81, P<0.049), KIRC (HR =1.63; 95% CI: 1.18–2.23, P=0.003), KIRP (HR= 3.55; 95% CI: 1.97–6.41, P<0.001), LGG (HR =1.94; 95% CI: 1.46–2.57, P<0.001), LIHC (HR =2.03; 95% CI: 1.51–2.73, P=0.001), LUAD (HR =1.36; 95% CI: 1.05–1.78, P=0.021), MESO (HR =2.59; 95% CI: 1.49–4.52, P=0.001), PAAD (HR =1.77; 95% CI: 1.20–2.62, P=0.004), PRAD (HR =2.25; 95% CI: 1.46–3.46, P=0.001), SARC (HR =1.58; 95% CI: 1.13–2.21, P=0.007), THCA (HR
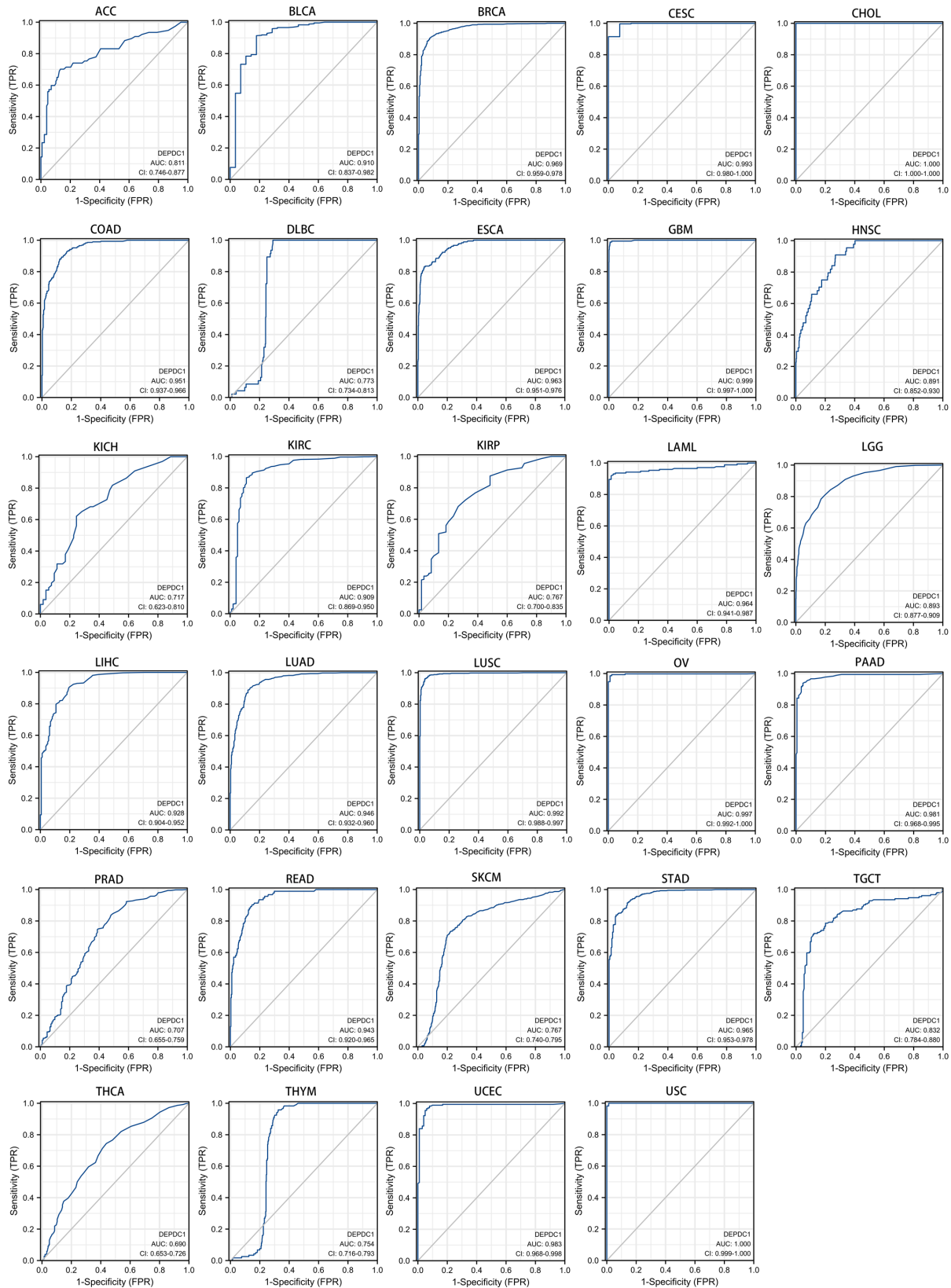
Figure 5 Diagnostic value of ROC analysis of *DEPDC1* in pan-cancer. ROC, receiver operating characteristic.
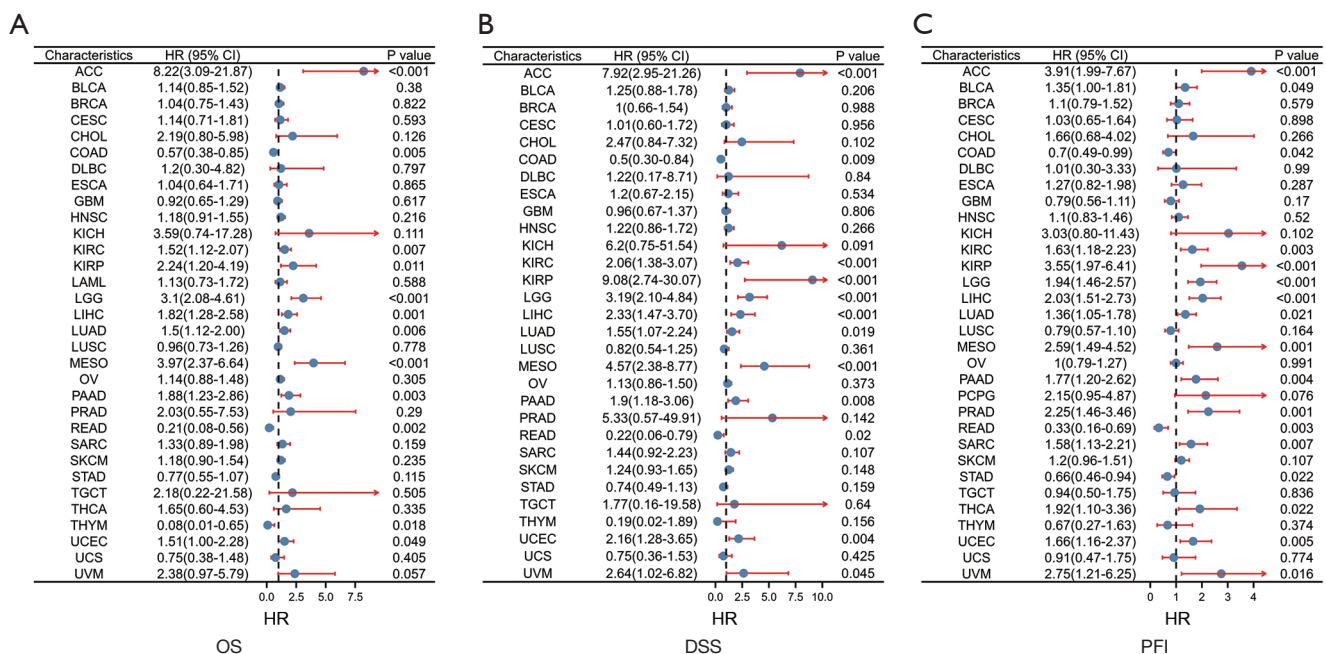

Figure 6 Univariate Cox regression and Kaplan-Meier overall survival analysis of *DEPDC1*. (A) The Forest map shows the univariate cox regression results of *DEPDC1* for OS in TCGA pan-cancer. (B) The Forest map shows the univariate cox regression results of *DEPDC1* for DSS in TCGA pan-cancer. (C) The Forest map shows the univariate cox regression results of *DEPDC1* for PFI in TCGA pan-cancer. HR, hazard ratio; OS, overall survival; DSS, disease-specific survival; PFI, progress free interval.

=1.92; 95% CI: 1.10–3.36, P=0.022), UCEC (HR =1.66; 95% CI: 1.16–2.37, P=0.005) and UVM (HR =2.75; 95% CI: 1.21–6.25, P=0.016). Higher DEPDC1 expression was associated with good PFI in cases of COAD (HR =0.7; 95% CI: 0.49–0.99, P=0.042), READ (HR =0.33; 95% CI: 0.16–0.69, P=0.003), and STAD (HR =0.66; 95% CI: 0.46–0.94, P=0.022) (*Figure 6C*). These results indicated that increased *DEPDC1* expression was associated with poor prognosis in a variety of tumor types, but in a few tumors they are associated with a good prognosis.

PPI network and GO and KEGG enrichment analyses

To investigate the functional mechanism of *DEPDC1* in carcinogenesis, we used the following parameters as screening conditions in the STRING (https://www.string-db.org/) database: active interaction sources ("Textmining, Experiments, Databases, Co-expression, Neighborhood, Gene Fusion, and Co-occurrence") and minimum required interaction score ["medium confidence (0.400)"] yielded the top 50 proteins interacting with *DEPDC1*. The results showed that the genes most associated with *DEPDC1* were kinesin family member 20A (*KIF20A*), DLG associated

protein 5 (*DLGAP5*), centromere protein F (*CENPF*), Rho GTPase activating protein 11A (*ARHGAP11A*), assembly factor for spindle microtubules (*ASPM*), kinesin family member 11 (*KIF11*), TTK protein kinase (*TTK*), BUB1 mitotic checkpoint serine/threonine kinase B (*BUB1B*), DNA topoisomerase II alpha (*TOP2A*), and zinc finger protein 224 (*ZNF224*) (*Figure 7A*). GO and KEGG pathway enrichment analyses of the 50 targeted binding proteins were obtained using the STRING tool. The results revealed that the proteins of interest were mainly involved in cell cycle, oncyte meiosis, progesterone-mediated oncyte maturation, cellular senescence, p53 signaling pathway, human immunodeficiency virus 1 infection, viral carcinogenesis, and FoxO signaling pathway. The main biological processes (BPs) were mitotic nuclear division, nuclear division, organelle fission, mitotic sister chromatid segregation, and sister c chromatid segregation. The main molecular functions (MFs) were microtubule binding, histone kinase activity, tubulin binding, chemokine activity, and motor activity. These results support the conclusion that *DEPDC1* is essential for tight junctions, cell cycle and nuclear division.
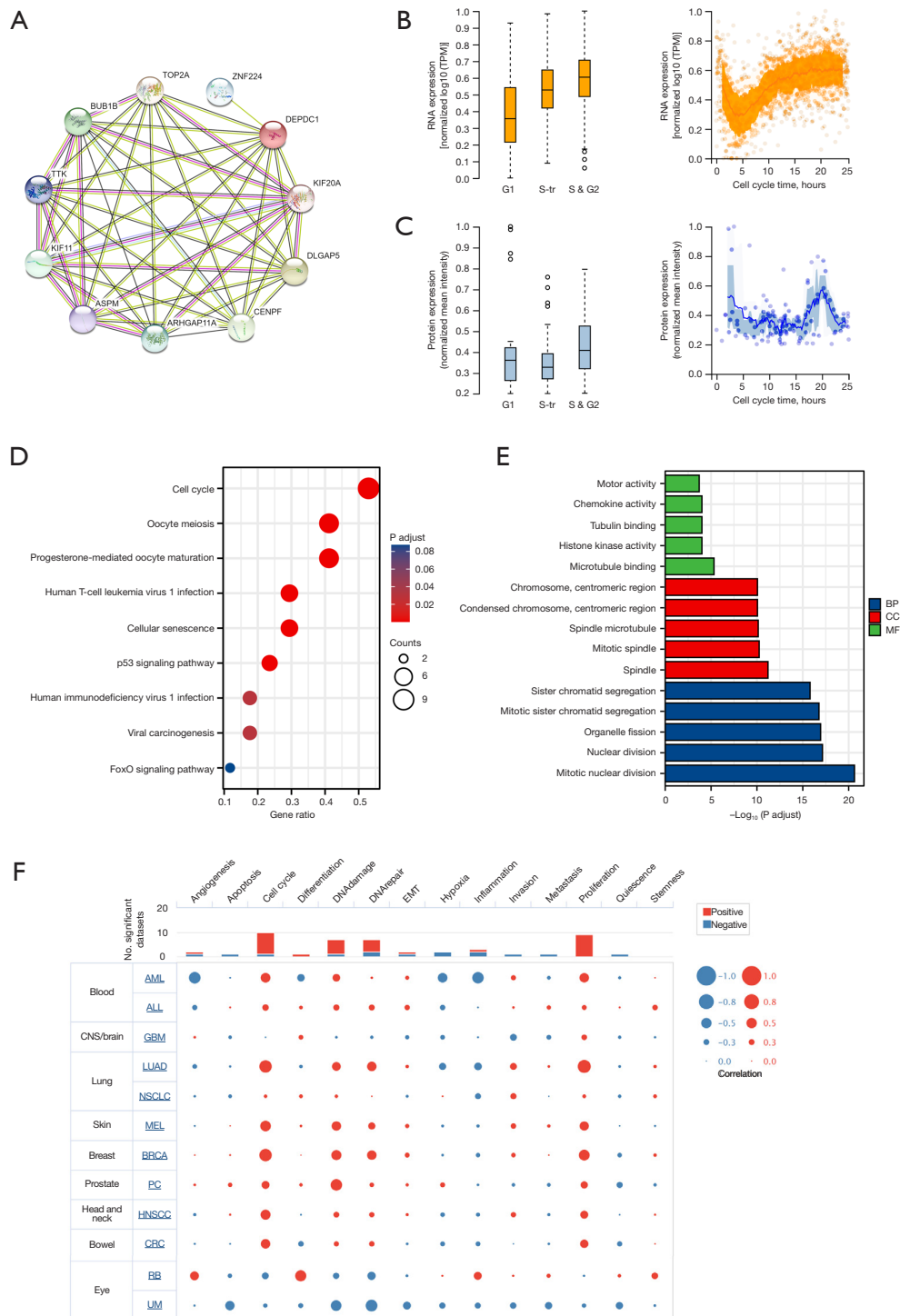
To determine whether the changes in *DEPDC1*

Figure 7 KEGG and GO enrichment analysis for *DEPDC1*. (A) The Protein-protein interaction (PPI) network of *DEPDC1* was constructed using the STRING database. (B, C) Plots of single-cell RNA-sequencing data from the FUCCI U-2 osteosarcoma cell line, showing the correlation between *DEPDC1* mRNA and protein expression and cell cycle progression. (D) KEGG analyses of *DEPDC1*. (E) GO analyses of DEGs. (F) *DEPDC1* significantly positively regulates cell cycle, DNA damage, DNA repair and proliferation by analysis of CancerSEA database. KEGG, Kyoto encyclopedia of genes and genomes; GO, Gene Ontology; BP, biological process; MF, molecular function; CC, cell component; DEGs, differentially expressed genes.

expression at the protein and transcript level were associated with the cell cycle, single-cell RNA-sequencing data from the human protein atlas (HPA) (https://www.proteinatlas.org/) (33) was analyzed. Fluorescent Ubiquitination-based Cell Cycle Indicator (FUCCI) revealed increased *DEPDC1* RNA and protein in U-2 OS cells expression in relation to cell cycle progression (*Figure 7B,7C*). To investigate the functions of the *DEPDC1* family in pan-cancer, we performed single-cell analysis using CancerSEA. The results indicated that *DEPDC1* positively regulated cell cycle, DNA damage, DNA repair, and proliferation in blood cancer, lung cancer, skin cancer, breast cancer, prostate cancer, HNSCC, and bowel cancer. These results suggested that *DEPDC1* is essential for cell cycle progression and proliferation of tumor cells (*Figure 7D-7F*).

Immune cell infiltration analyses

Immune infiltration of tumors is the frontier direction of current tumor research, and thus, identifying valuable biomarkers of tumor immune infiltration is crucial. To determine whether *DEPDC1* could serve as a pan-cancer marker of immune infiltration, we explored the association of *DEPDC1* with various immune cells in human cancers using XCELL metrics in TIMER2.0 (*Figure 8A*). The results showed that the expression level of DEPDC1 was positively correlated with CD4$^+$ T helper 2 (Th2) cells and common lymphoid progenitors. Correspondingly, there was a negative correlation between the expression level of *DEPDC1* and natural killer (NK) T cells, CD4$^+$ central memory T cells and CD4$^+$ effector memory T cells. In most cancers, except TGCT, THYM, and UCS, robust and significant relationships existed between *DEPDC1* expression and expression levels of recognized immune checkpoints including interleukin 10 receptor subunit beta (*IL10RB*), *CD274*, transforming growth factor beta receptor 1 (*TGFBR1*), kinase insert domain receptor (*KDR*), and programmed cell death 1 ligand 2 (*PDCD1LG2*). This suggested a potential synergy of *DEPDC1* with known immune checkpoints (*Figure 8B*).

DEPDC1 is upregulated in OSCC and has prognostic value

It is well-documented that *DEPDC1* is upregulated in a variety of tumors and is associated with poor prognosis. To verify this, we analyzed the expression of *DEPDC1* and its prognostic value in OSCC. As shown in *Figure 9A,9B*,

both paired and unpaired analyses in TCGA-OSCC showed that the mRNA expression level of *DEPDC1* was significantly upregulated. *DEPDC1* was also associated with poor prognosis in OSCC (*Figure 9C*), and the expression of *DEPDC1* in OSCC can be used to differentiate normal and tumor tissues (*Figure 9D*). Tumor samples with low expression of *DEPDC1* in OSCC had higher immune score, stromal score, and ESTMATE score, indicating that *DEPDC1* inhibited immune infiltration in OSCC (*Figure 9E*). In addition, using the single sample gene set enrichment analysis (ssGSEA) method, we found that *DEPDC1* was significantly positively correlated with Th2 cells and T helper cells, and significantly negatively correlated with presenting cells, which is consistent with our analysis in pan-cancer (*Figure 9F*). To further confirm the abnormally high expression of *DEPDC1* in OSCC, we collected 57 OSCC samples and 12 normal samples, and analyzed the expression of *DEPDC1* after IHC staining of these samples. The results showed that *DEPDC1* was indeed significantly upregulated in OSCC (*Figure 9G-9H*).

Discussion

Cancer presents a global threat to health and screening for valuable diagnostic and therapeutic biomarkers is crucial. *DEPDC1* is a highly evolutionarily conserved gene that is widely expressed in animals and plants in nature (18,21). Current studies have shown that *DEPDC1* has orthologs in 304 organisms and humans (13,16,34). In humans, the *DEPDC1* gene is a novel oncogene located on chromosome 1 (21). At present, research related to the function of *DEPDC1* is still in its infancy. Furthermore, the role of DEPDC1 in pan-cancer has not been reported. This project evaluated DEPDC1 expression changes in pan-cancer. Analysis of the sequencing data of 33 tumors and corresponding normal samples obtained from the TCGA and GTEx databases revealed that *DEPDC1* was significantly upregulated in 29 human cancers, including ACC, BRCA, BLCA, CESC, COAD, CHOL, DLBC, ESCA, GBM, HNSC, KIRP, KIRC, KICH, LUSC, LUAD, LIHC, LGG, OV, PCPG, PRAD, PAAD, READ, SKCM, STAD, SARC, THYM, THCA, UCS, and UCEC. Meanwhile, *DEPDC1* was significantly downregulated in LAML and TGCT. This finding suggested that *DEPDC1* is abnormally amplified in most malignancies and acts as a proto-oncogene and may be involved in tumorigenesis or cancer development.

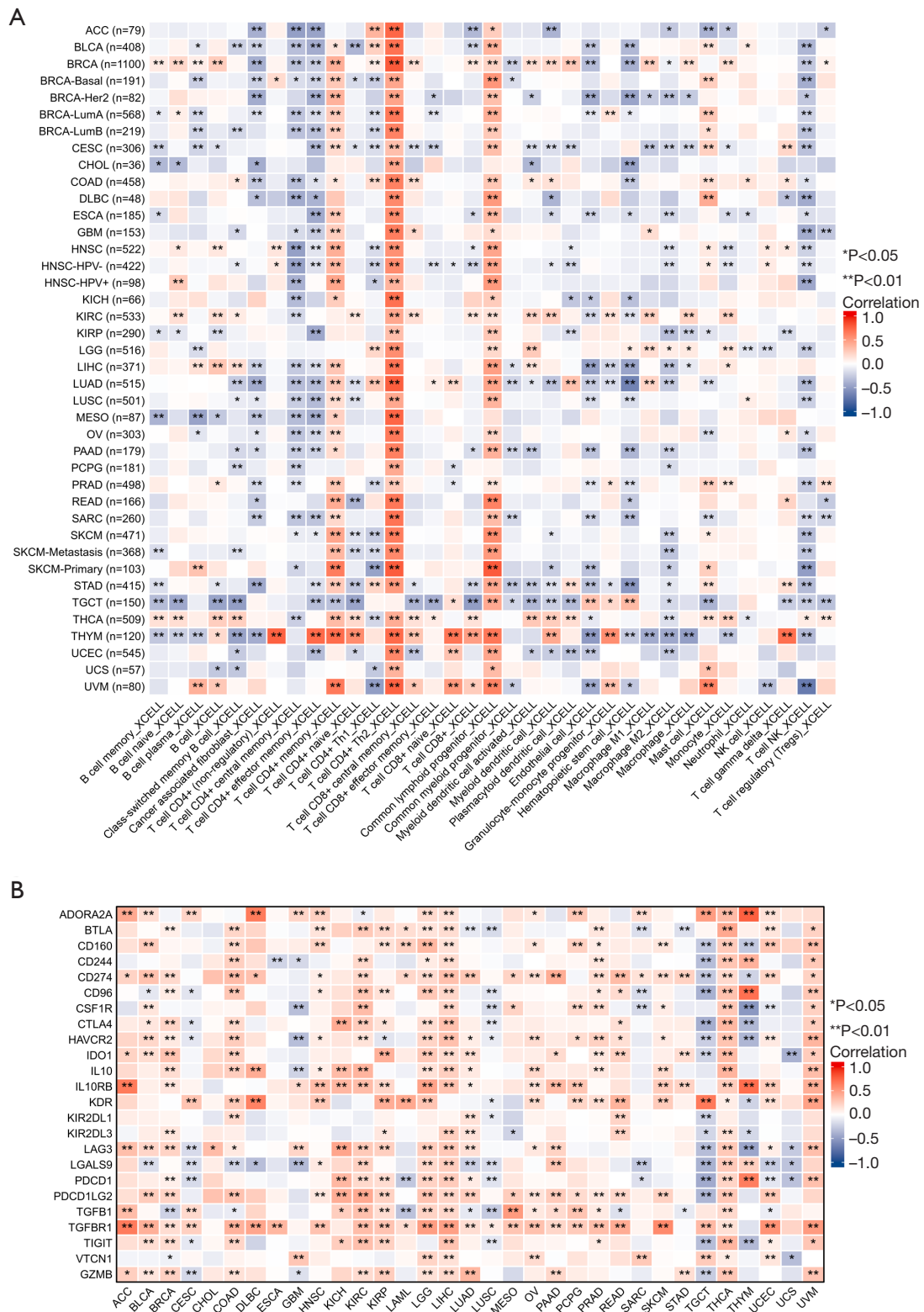The determination of the immune subtype of tumors

Figure 8 Analysis of the relationship between *DEPDC1* and immune cell infiltration. (A) The correlation between *DEPDC1* and 35 kinds of XCELL immune cells in pan-cancer was analyzed by TIMER2 database. (B) Correlation of expression levels of *DEPDC1* with currently identified immune checkpoints.
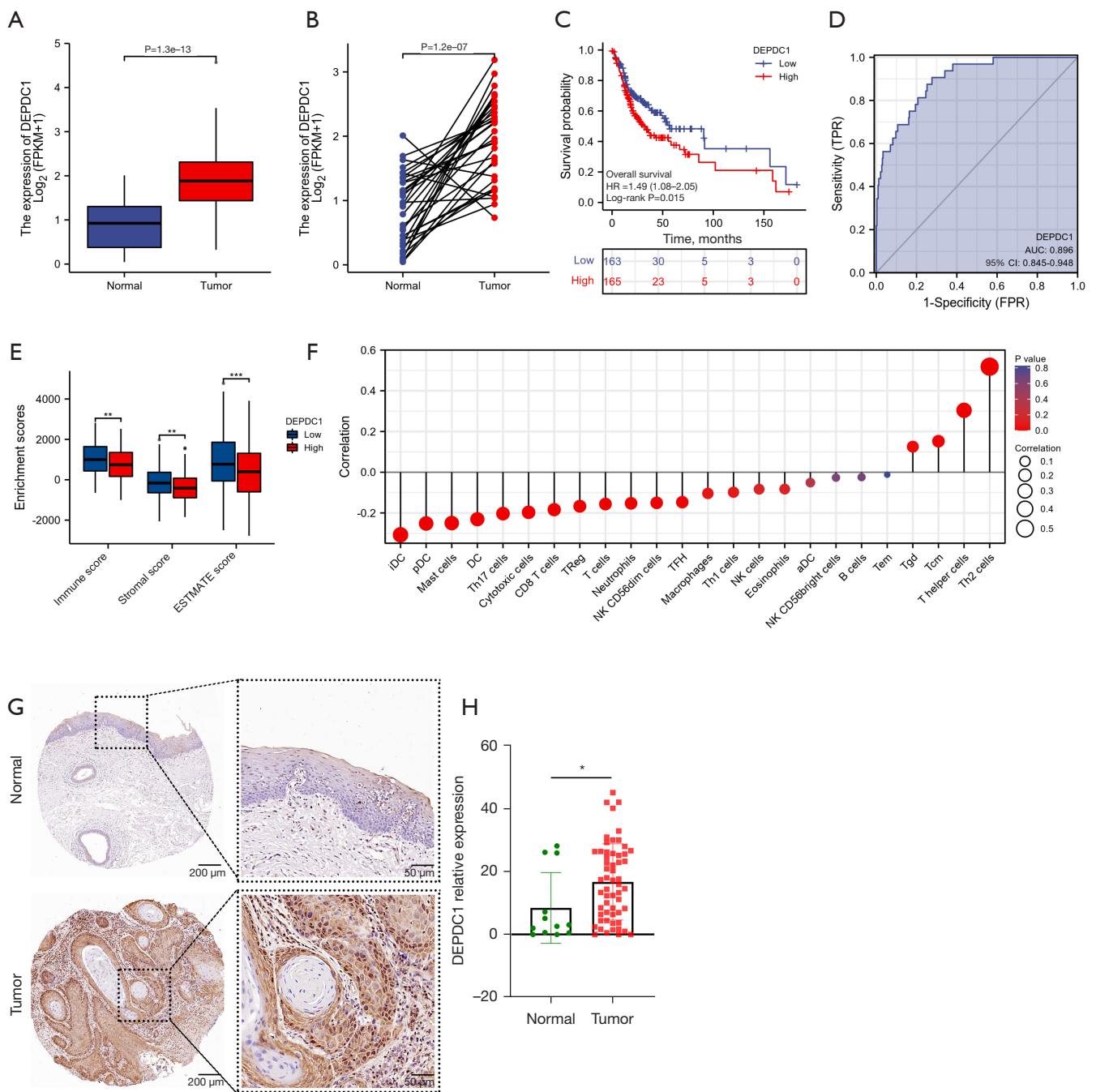
Figure 9 Analysis of *DEPDC1* expression and prognosis in OSCC. (A) Unpaired comparison of *DEPDC1* expression in TCGA-OSCC. (B) Pairwise comparison of *DEPDC1* expression in TCGA-OSCC. (C) Analysis of the prognostic value of *DEPDC1* in OSCC. (D) Diagnostic value of ROC analysis of *DEPDC1*. (E) Comparison of immune score, stromal score and ESTMATE score between *DEPDC1* high and low expression groups. (F) ssGSEA analysis of the correlation between *DEPDC1* and immune cells in OSCC. (G,H) IHC staining of *DEPDC1* protein expression in OSCC and normal samples. *P<0.05; **P<0.01; ***P<0.001. TCGA, The Cancer Genome Atlas; ssGSEA, single sample gene set enrichment analysis; OSCC, oral squamous cell carcinoma; single sample gene set enrichment analysis; IHC, immunohistochemistry; ROC, receiver operating characteristic; AUC, area under the curve; FPKM, fragments per kilobase of exon model per million mapped fragments; FPR, false positive rate; TPR, true positive rate.

is the basis for personalized and precise treatment of tumors. Our results showed that *DEPDC1* is significantly differentially expressed in different immune subtypes of 23 cancers, including ACC, BLCA, BRCA, COAD, ESCA, GBM, KIRC, KIRP, LGG, LIHC, LUAD, LUSC, MESO, OV, PAAD, PRAD, READ, SARC, SKCM, STAD, TGCT, THCA, and UCEC. It is worth noting that *DEPDC1* expression was the lowest in the C3 and C5 subtypes. Immunological landscape studies on cancer have shown that C3 (inflammatory subtype) and C5 (immune quiet subtype) have better survival outcomes than other immune subtypes (35). These results suggested that *DEPDC1* as a proto-oncogene is associated with a poor prognosis. At the same time, *DEPDC1* expression levels were also significantly different in molecular subtypes of 13 cancer types, including KIRP, BRCA, LUSC, COAD, UCEC, LIHC, READ, ACC, OV, PRAD, PCPG, LGG, and STAD. This suggested that *DEPDC1* may be a key indicator of tumor immune subtype or molecular typing. Therefore, taking the immune subtype or molecular subtype of the tumor as a starting point may help to understand the role of *DEPDC1* in pan-cancer.

To evaluate the value of *DEPDC1* as a diagnostic and prognostic marker in pan-cancer, we performed ROC curve analysis on pan-cancer and found that *DEPDC1* can effectively distinguish normal and tumor samples in all types of cancers (AUC >0.7), especially in CESC, CHOL, LUSC, OV, and UCS (AUC >0.99). Furthermore, pan-cancer survival analysis revealed that DEPDC1 was significant in OS, DSS, and PFI in ACC, COAD, KIRP, KIRC, LGG, LUAD, LIHC, MESO, PAAD, READ, THYM, and UCEC. These results suggested that *DEPDC1* has an extremely important diagnostic value in pan-cancer and can be used as a prognostic marker in specific cancers. Therefore, *DEPDC1* can be used as a potential biomarker or therapeutic target for precision medicine of tumors in the future.

To gain an in-depth understanding of the biological function of *DEPDC1*, we obtained 50 interacting proteins of *DEPDC1* through the STRING database for GO and KEGG pathway enrichment analysis. The analysis revealed that *DEPDC1* is mainly involved in cell cycle, cell meiosis, and progesterone-mediated cell cycle, as well as maturation, cellular senescence, *p53* signaling, human immunodeficiency virus 1 infection, viral carcinogenesis, and *FoxO* signaling. The associated BPs were primarily involved in the mitotic nuclear division, nuclear division, organelle fission, mitotic sister chromatid segregation, and sister c chromatid segregation. The main enriched MFs were microtubule

binding, histone kinase activity, tubulin binding, chemokine activity, and motor activity. These results suggested that *DEPDC1* is essential for cell cycle regulation and regulates nuclear division in cells. This is consistent with the results of existing functional studies related to *DEPDC1* (12,22,36).

In addition to the involvement of *DEPDC1* in regulating the cell cycle, the results herein demonstrated that *DEPDC1* expression is highly correlated with immune infiltration. Through the TIMER2.0 database, we found that DEPDC1 was significantly associated with the abundance of 35 XCELL immune infiltrating cells in pan-cancer. In particular, *DEPDC1* was a significant positive correlation with CD4⁺ Th2 cells and common lymphoid progenitor cells. Conversely, DEPDC1 was significantly negatively correlated with NK cells, CD4⁺ central memory T cells, and CD4⁺ effector memory T cell. These results suggested that *DEPDC1* can activate tumor immune escape through the combined action of activating Th2 cells and inhibiting NK cells, thereby enabling tumor cells to obtain a more stable environment to deteriorate the body's health.

Cancer patients usually do not have a significant reduction in T cell numbers, but most of the T cell function is lost, which is often referred to as T cell exhaustion (37). T cell exhaustion is usually accompanied by enhanced *PD-1* expression on the surface of T cells, and a large amount of *PDL1* and *PDL2* expressed on the surface of the corresponding tumor cells. We found that DEPDC1 positively correlated with T cell exhaustion marker genes such as *CD274*, *TGFBR1*, *KDR*, *PDCD1LG2*, *GZMB*, and *LAG2* in pan-cancer. This suggested that *DEPDC1* may be involved in suppressing tumor immunity by interacting with immune checkpoints.

There were some limitations to this study. This investigation used public databases including TCGA to explore the relationship between *DEPDC1* and pan-cancer. Although clinical samples from our hospital were used for verification, further clinical data should be analyzed to confirm these results. The biological functions associated with *DEPDC1* were determined by bioinformatics, and future experiments involving *in vitro* and *in vivo* experiments are warranted.

Conclusions

In conclusion, the results herein revealed that *DEPDC1* is up-regulated in pan-cancer tissues, with the exception of LAML and TGCT, and plays an immune-oncogenic role in pan-cancer. Indeed, *DEPDC1* can be used as a broad-

spectrum biomarker for the diagnosis and therapeutic of pan-cancer.

Footnote

Reporting Checklist: The authors have completed the REMARK reporting checklist. Available at https://atm.amegroups.com/article/view/10.21037/atm-22-5598/rc

Data Sharing Statement: Available at https://atm.amegroups.com/article/view/10.21037/atm-22-5598/dss

Conflicts of Interest: All authors have completed the ICMJE uniform disclosure form (available at https://atm.amegroups.com/article/view/10.21037/atm-22-5598/coif). The authors have no conflicts of interest to declare.

Ethical Statement: The authors are accountable for all aspects of the work in ensuring that questions related to the accuracy or integrity of any part of the work are appropriately investigated and resolved. The study was conducted in accordance with the Declaration of Helsinki (as revised in 2013). The study was approved by the Ethics Committee of School of Life Sciences, Central South University (No. 2022-1-44) and informed consent was taken from all the patients.

References

1. Mattiuzzi C, Lippi G. Current Cancer Epidemiology. J Epidemiol Glob Health 2019;9:217-22.
2. Siegel RL, Miller KD, Fuchs HE, et al. Cancer Statistics, 2021. CA Cancer J Clin 2021;71:7-33.
3. Rizvi S, Khan SA, Hallemeier CL, et al. Cholangiocarcinoma - evolving concepts and therapeutic strategies. Nat Rev Clin Oncol 2018;15:95-111.
4. Weiss SA, Wolchok JD, Sznol M. Immunotherapy of Melanoma: Facts and Hopes. Clin Cancer Res 2019;25:5191-201.
5. Zhou X, Du J, Liu C, et al. A Pan-Cancer Analysis of CD161, a Potential New Immune Checkpoint. Front Immunol 2021;12:688215.
6. Zeng D, Ye Z, Wu J, et al. Macrophage correlates with immunophenotype and predicts anti-PD-L1 response of urothelial cancer. Theranostics 2020;10:7002-14.
7. Cao R, Yang F, Ma SC, et al. Development and interpretation of a pathomics-based model for the prediction of microsatellite instability in Colorectal Cancer. Theranostics 2020;10:11080-91.
8. Emens LA. Breast Cancer Immunotherapy: Facts and Hopes. Clin Cancer Res 2018;24:511-20.
9. Shen J, Xi M. DEPDC1 is Highly Expressed in Lung Adenocarcinoma and Promotes Tumor Cell Proliferation. Zhongguo Fei Ai Za Zhi 2021;24:453-60.
10. Wang Q, Li A, Jin J, et al. Targeted interfering DEP domain containing 1 protein induces apoptosis in A549 lung adenocarcinoma cells through the NF-κB signaling pathway. Onco Targets Ther 2017;10:4443-54.
11. Liu C, Li X, Hao Y, et al. STAT1-induced upregulation of lncRNA KTN1-AS1 predicts poor prognosis and facilitates non-small cell lung cancer progression via miR-23b/DEPDC1 axis. Aging (Albany NY) 2020;12:8680-701.
12. Gong Z, Chu H, Chen J, et al. DEPDC1 upregulation promotes cell proliferation and predicts poor prognosis in patients with gastric cancer. Cancer Biomark 2021;30:299-307.
13. Zhou C, Wang P, Tu M, et al. DEPDC1 promotes cell proliferation and suppresses sensitivity to chemotherapy in human hepatocellular carcinoma. Biosci Rep 2019;39:BSR20190946.
14. Amisaki M, Yagyu T, Uchinaka EI, et al. Prognostic Value of DEPDC1 Expression in Tumor and Non-tumor Tissue of Patients With Hepatocellular Carcinoma. Anticancer

Res 2019;39:4423-30.

15. Guo W, Li H, Liu H, et al. DEPDC1 drives hepatocellular carcinoma cell proliferation, invasion and angiogenesis by regulating the CCL20/CCR6 signaling pathway. Oncol Rep 2019;42:1075-89.

16. Harada Y, Kanehira M, Fujisawa Y, et al. Cell-permeable peptide DEPDC1-ZNF224 interferes with transcriptional repression and oncogenicity in bladder cancer cells. Cancer Res 2010;70:5829-39.

17. Kanehira M, Harada Y, Takata R, et al. Involvement of upregulation of DEPDC1 (DEP domain containing 1) in bladder carcinogenesis. Oncogene 2007;26:6448-55.

18. Zhao H, Yu M, Sui L, et al. High Expression of DEPDC1 Promotes Malignant Phenotypes of Breast Cancer Cells and Predicts Poor Prognosis in Patients With Breast Cancer. Front Oncol 2019;9:262.

19. Huang L, Chen K, Cai ZP, et al. DEPDC1 promotes cell proliferation and tumor growth via activation of E2F signaling in prostate cancer. Biochem Biophys Res Commun 2017;490:707-12.

20. Wang Q, Jiang S, Liu J, et al. DEP Domain Containing 1 Promotes Proliferation, Invasion, and Epithelial-Mesenchymal Transition in Colorectal Cancer by Enhancing Expression of Suppressor of Zest 12. Cancer Biother Radiopharm 2021;36:36-44.

21. Kharrat A, Millevoi S, Baraldi E, et al. Conformational stability studies of the pleckstrin DEP domain: definition of the domain boundaries. Biochim Biophys Acta 1998;1385:157-64.

22. Feng X, Zhang C, Zhu L, et al. DEPDC1 is required for cell cycle progression and motility in nasopharyngeal carcinoma. Oncotarget 2017;8:63605-19.

23. Gao J, Aksoy BA, Dogrusoz U, et al. Integrative analysis of complex cancer genomics and clinical profiles using the cBioPortal. Sci Signal 2013;6:pl1.

24. Cerami E, Gao J, Dogrusoz U, et al. The cBio cancer genomics portal: an open platform for exploring multidimensional cancer genomics data. Cancer Discov 2012;2:401-4.

25. Vivian J, Rao AA, Nothaft FA, et al. Toil enables reproducible, open source, big biomedical data analyses.

26. Li T, Fu J, Zeng Z, et al. TIMER2.0 for analysis of tumor-infiltrating immune cells. Nucleic Acids Res 2020;48:W509-14.

27. Li B, Severson E, Pignon JC, et al. Comprehensive analyses of tumor immunity: implications for cancer immunotherapy. Genome Biol 2016;17:174.

28. Aran D, Hu Z, Butte AJ. xCell: digitally portraying the tissue cellular heterogeneity landscape. Genome Biol 2017;18:220.

29. Ru B, Wong CN, Tong Y, et al. TISIDB: an integrated repository portal for tumor-immune system interactions. Bioinformatics 2019;35:4200-2.

30. Yuan H, Yan M, Zhang G, et al. CancerSEA: a cancer single-cell state atlas. Nucleic Acids Res 2019;47:D900-8.

31. Hu X, Xia K, Xiong H, et al. G3BP1 may serve as a potential biomarker of proliferation, apoptosis, and prognosis in oral squamous cell carcinoma. J Oral Pathol Med 2021;50:995-1004.

32. Chen Y, Sun Z, Chen W, et al. The Immune Subtypes and Landscape of Gastric Cancer and to Predict Based on the Whole-Slide Images Using Deep Learning. Front Immunol 2021;12:685992.

33. Colwill K; ; Gräslund S. A roadmap to generate renewable protein binders to the human proteome. Nat Methods 2011;8:551-8.

34. Ramalho-Carvalho J, Martins JB, Cekaite L, et al. Epigenetic disruption of miR-130a promotes prostate cancer by targeting SEC23B and DEPDC1. Cancer Lett 2017;385:150-9.

35. Thorsson V, Gibbs DL, Brown SD, et al. The Immune Landscape of Cancer. Immunity 2018;48:812-830.e14.

36. Mi Y, Zhang C, Bu Y, et al. DEPDC1 is a novel cell cycle related gene that regulates mitotic progression. BMB Rep 2015;48:413-8.

37. Jiang W, He Y, He W, et al. Exhausted CD8+T Cells in the Tumor Immune Microenvironment: New Pathways to Therapy. Front Immunol 2020;11:622509.

Nat Biotechnol 2017;35:314-6.

(English Language Editor: J. Teoh)